

Analytical methodology of Seismic Fragility Curve for Reinforcement Concrete Pier Bridges in Egypt

Islam M. Ezz El-Arab

Abstract— A seismic vulnerability evaluation method based on structural analysis for RC bridges with simple pier bents is proposed in the paper. The proposed method is based on the hypothesis of the flexible pier-rigid deck behavior of the structure subjected to transversal seismic loads. A flexible pier-rigid deck simplified model was therefore developed. This model has been chosen after verifying the correlation between the responses of the proposed model and of the real structure which was presented by Egyptian General Authority of Roads and Bridges. The damage produced by the earthquake load is centered on the piers of the bridge, while the dynamic study of the deck can be performed after the structural analysis of the piers in an uncoupled way. The maximum damage of the piers under seismic actions is the principal aim of the proposed structural evaluation methodology. A damage index is used for this purpose, which describes the state of the material at each point of the structure. The study success to present the fragility curves which show that the peak ground acceleration for 50% probability of exceeding slight, moderate and sever damage ranges from approximately 0.15 to 0.4 g for this typical and repeated RC bridge in Egypt.

Keywords: Analytical methodology, Fragility curve, Egypt, RC bridges, Seismic analysis.

I. INTRODUCTION

Fragility curves describe the probability of a structure being damaged beyond a specific damage state for various levels of ground excitation. This can be used for prioritizing retrofit, pre-earthquake planning, and loss estimation tools. This is particularly useful in regions of moderate and slightly seismicity, such as Egypt and the Middle East area, where Egyptian General Authority of Roads and Bridges (EGARB) are being to develop retrofit programs, in addition to conducting pre-earthquake planning.

In the recent years, Seismic vulnerability assessment and development of fragility curves for existing bridges are a matter of great concern by the researchers, [1-4]. Fragility curves of bridges can be developed empirically as well as analytically. Empirical fragility curves are usually developed based on the damage reports from past earthquakes. When actual bridge damage and ground motion data are not

available, analytical fragility curves can be used to assess the performance of bridges, [5-7].

Current methods for evaluating seismic damage to bridges was divided into four main groups by (Park and Ang, Charney)[8,9]: (1) obtaining of a vulnerability index by means of inspection; (2) evaluation of the damage through structural analysis; (3) estimation of vulnerability based on expert's judgment and (4) statistical analysis of actual data. The first method is based on simple evaluations aimed simply at providing a classification of those structures which show greatest seismic vulnerability. Models based on structural analysis provide a greater quantity of results, but reliability depends on their capacity to represent real seismic behavior. Evaluation based on expert's judgment requires a large number of professionals with in-depth knowledge of the problem and proven experience, while statistical evaluations based on real damage data can only be applied in zones of moderate or high seismicity where sufficient data are available.

In this respect, due to the lack of information from past earthquakes damage on bridges, it is not possible to derive fragility curves empirically for the typical bridge piers in Egypt. Therefore, fragility curves have been developed analytically from non linear dynamic analyses of typical bridge piers. Since damage states are mostly related to structural capacity (C) and the ground motion intensity parameter is related to structural demand (D), the Damage Index (DI) gives the probability that the seismic demand will exceed the structural capacity. Mander and Basoz [10], have presented the theory of fragility curves for highway bridges based on uncertainties in various bridge parameters to evaluate seismic vulnerability of typical bridges. While Ghobarah et al. [11], have quantified numerically the damage states from the dynamic responses of the bridges under various levels of ground motion excitation; Hwang et al. [12], described a detailed procedure for analytical development of fragility curves.

The main objective of this study is to find analytical fragility curves for typical Egyptian reinforced concrete bridge piers based on numerical approach taking into account, the structural parameters and the variation of the input ground motion. Prior to the newly established Egyptian loading seismic regulation code for the structures building and bridges (ECP 201(1993,2003, and 2008))[13], the bridge piers have been designed using the seismic design coefficient method (Amplification Dynamic effect factor I).

Manuscript published on 30 December 2012.

* Correspondence Author (s)

Islam Ezz El-Arab, Structural Engineering Department, Tanta University/ Faculty of Engineering, Tanta, Egypt.

© The Authors. Published by Blue Eyes Intelligence Engineering and Sciences Publication (BEIESP). This is an [open access](http://creativecommons.org/licenses/by-nc-nd/4.0/) article under the CC-BY-NC-ND license <http://creativecommons.org/licenses/by-nc-nd/4.0/>.

Analytical methodology of Seismic Fragility Curve for Reinforcement Concrete Pier Bridges in Egypt

In this respect, seismic coefficients equal to 20% of the total live load in the horizontal direction and 7% of the total live load in the vertical direction have been used to design the bridge piers. By using worldwide strong motion records, the damage indices as defined by Park and Ang [8], are obtained through a non-linear dynamic response analysis. The obtained damage indices defined for five damage rank and the ground motion indices are then combined to derive the corresponding fragility curves for the reinforced concrete bridge piers, as presented in Table 1.

Table 1 Relationship between the damage index (DI), and damage rank (DR), [8].

Definition	Damage rank	Damage index
No damage	D	$0.00 < DI \leq 0.14$
Slight damage	C	$0.14 < DI \leq 0.40$
Moderate	B	$0.40 < DI \leq 0.60$
Extensive	A	$0.60 < DI \leq 1.00$
Complete	As	$1.00 \leq DI$

II. BRIDGE CONFIGURATION

The bridge detail was presented by Egyptian General Authority of Roads and Bridges (EGARB), which was used in all most medium and large bridges on road intersection or river Nile bridges. The bridge is a continuous, four-simple support spans, box girder structure. The three intermediates bents consist of three piers.

The bridge configuration is cleared as shown in Fig. 1, and its properties were listed in Table 2. The substructure of bridge consists of rigid abutments at the ends in addition to reinforcement concrete piers. The overall length of bridge is 116.0 m. the superstructure consists of reinforcement concrete deck slab of 12.0 m wide. Three intermediate reinforcement concrete wall pier.

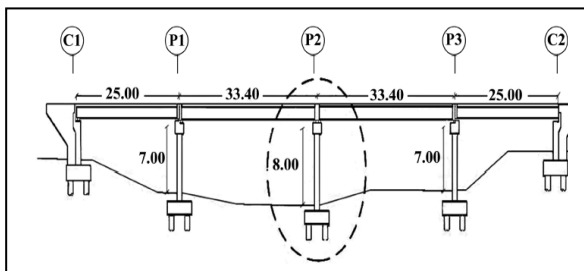


Fig. 1 The configuration of continues simple support of the reinforcement concrete bridge, (EGARB).

Table 2 The geometry and dynamic characteristics as per presented by (EGARB).

Bridge properties	value
Span length, (m)	$(2 \times 25.0 + 2 \times 33.0) = 116.0$ m
Wall pier shape (Rectangular) (5.0x1.0)m	
Steel reinforcement of each pier	33T32 (main vertical steel) T12 @ 20 cm (Hoops)
Wall pier high, (m)	(7.0 and 8.0)
Pier wall Area, (m ²)	$(5.0 \times 1.0) = 8.0$
Second moment of inertia of wall pier in transversal direction, (m ⁴)	10.417

Fundamental time period of bridge in transversal direction, (sec.)	0.318
--------------------------------------------------------------------	-------

The paper presents two methods of bridge simulation. The first simulation is accurate finite element model by three dimensional modeling using professional computer code, DRAIN-2DX [14], while the second was developed based on the mathematical simplified proposal which will be explained in details in the below section to be simpler. The verification will be presented between two simulation methods.

The sectional analysis of bridge pier is carried out by using the software package RESPONSE-2000 [15], for two reasons using: (1) to find out the two possible failure modes, i.e., shear or flexural failure modes of the bridge piers and (2) to obtain the force–displacement relationship at the top of the bridge piers, which is necessary for the nonlinear analysis. In this respect, the cross sectional dimension of the pier bridge, the yield strength of steel σ_{sy} , the compressive strength concrete σ_c , the diameter of longitudinal reinforcement bars as well as the reinforcement bars are taken as input parameters. Fig. 2 shows the moment curvature curve of the bridge pier.

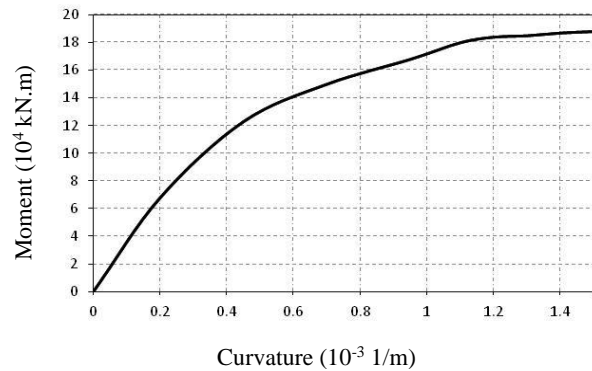


Fig. 2 Moment curvature curve for the pier bridge.

III. INPUT GROUND EXCITATION

Three different ground excitations are selected to match the seismicity of Egypt. One of them is Al-Aqba earthquake, 1995 which shocked east of Egypt (Al-Aqba Gulf), in 1995, and others two national earthquakes are El-Centro, 1940, and Northridge, 1994; two of this ground excitation naturally has maximum scaled spectrum acceleration. Figs. 3a, b show the acceleration time history of the three earthquakes ground excitation Al-Aqba, 1995, El-Centro, 1940, Northridge 1994, in longitudinal and transversal direction, respectively. Both of El-Centro, 1940 and Northridge, 1994 are scaled to match the seismic requirements for the zone of case study as it is cleared in Figs. 3c and 3d. This scaling of earthquake ground acceleration will make the results comparison from others dynamic and an equivalent static load are more rational and fair judged comparison for the Egypt zone. The peak ground acceleration which was used has a motions ranges from 0.07 to 0.6 g. this range is suitable and compatible to the microzonation map of seismicity characteristic in Egypt area.



IV. SIMPLIFIED ELASTIC MODEL FOR RC BRIDGES

A detailed analysis of the bridge inventory in the Egyptian General Authority of Roads and Bridges (EGARB), shows approximately 90% of bridges in Egypt are multi-span simply supported girder bridges, multi-span continuous girder bridges, which presented in the study.

RC bridges with simple pier bents have greater redundancy and strength in their longitudinal direction; therefore greater damage will occur in piers when they are subjected to transversal excitation. Consequently, the proposed model is developed for the study of the response of bridges subjected to earthquakes acting in a transversal direction to that of the

bridge axis. The simplified model shown in Fig. 4a, where it is based on the following hypotheses:

1. The piers are modeled as continuous elements with distributed mass and infinite axial stiffness.
2. The girders are modeled as perfectly stiff elements concentrating the mass at the top of the piers.
3. The soil-structure interaction effect in piers and abutments is considered by means of linear springs that represent the rotational stiffness of the soil.
4. The abutments are considered to be perfectly stiff.

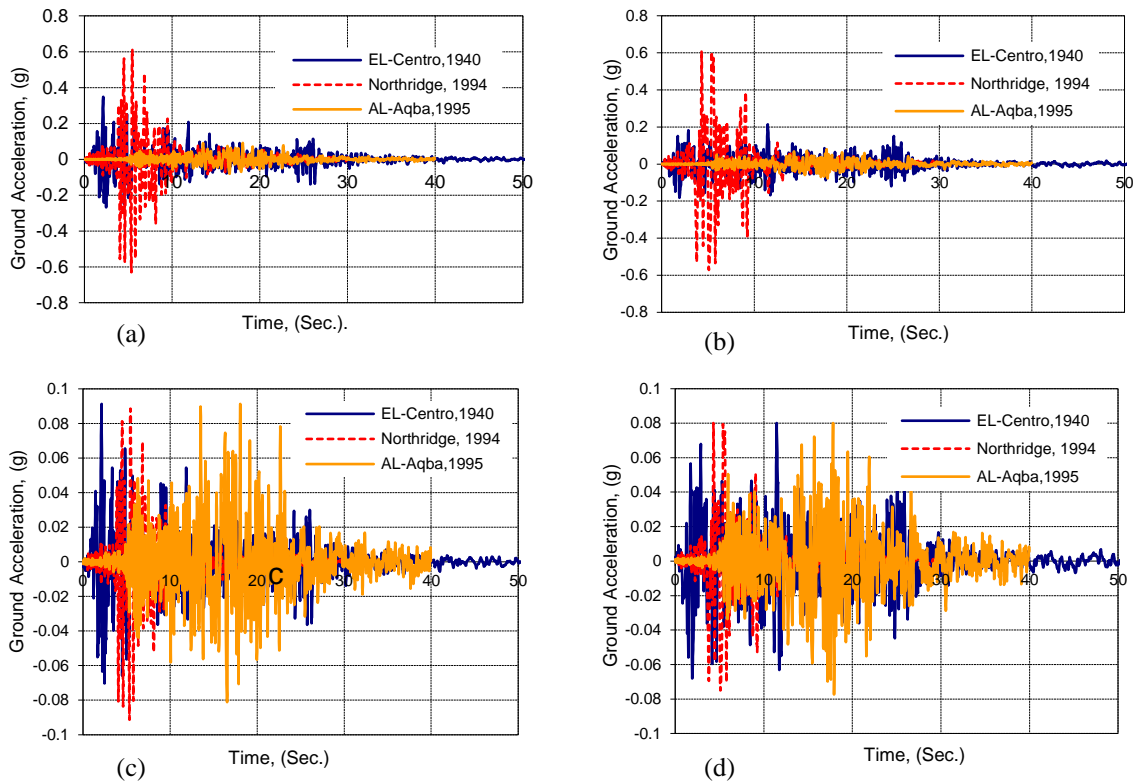


Fig. 3 Un-Factored time history ground acceleration of earthquakes in (a) longitudinal, (b) transversal direction, and Factored time history ground acceleration of earthquakes in (c) longitudinal, (d) transversal direction, respectively.

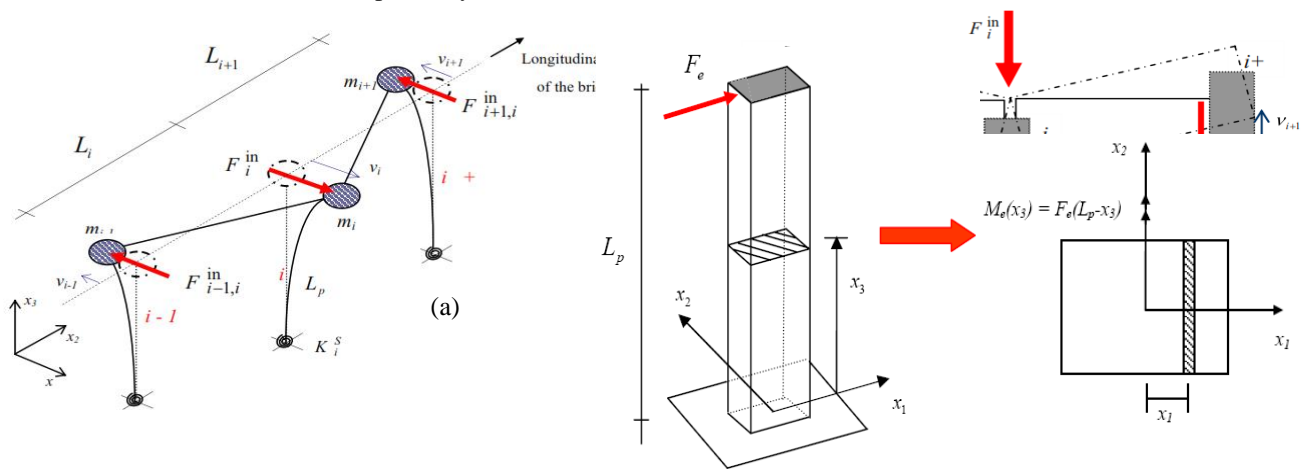


Fig. 4 (a) Basic scheme for the analysis of the bridge, (b) Girder rotation produced by the displacements at the top of the piers, and (c) Simplified model of a pier used in the non-linear analysis, respectively.

Accordingly, the transversal displacements at the top of the piers are the only degrees of freedom of the structural system.

The displacement of pier “i” generates the force distribution indicated in Fig. 4b, where F_{in} is the inertia force, $F_{i,i-1}$ and $F_{i,i+1}$ are the elastic forces produced by the rotation of the girders adjacent to pier i, and $F_{i-1,i}$ and $F_{i+1,i}$ are the elastic forces produced in the piers (i-1) and (i+1), respectively by the rotation of the contiguous girders. That is, for the pier under study, the sub-index indicates the pier on which the forces acted and the associated pier with it has the same girder. As it can be observed in Fig. 4b, the worst condition occurs when the two adjacent piers are displaced in the opposite direction to that of the displacement of pier i.

The bearings on each pier of the bridge are simulated as short columns with a rectangular cross section, whose behavior is governed mainly by shear deformations. The influence of the bearings on the behavior of the bridge is associated with their shear modulus, G , the distance in plan between the geometric centers of the bearings of each pier, h_a , their height, a , and the area of their cross section, A_p . On the basis of the above mentioned hypotheses, the total elastic force, R_i , due to the rotation of the adjacent girders to pier i is

$$R_i = F_{i,i-1} + F_{i,i+1} = \left[\frac{GA_p h_a^2}{aL_i^2} + \frac{GA_p h_a^2}{aL_{i+1}^2} \right] v_i - \left[\frac{GA_p h_a^2}{aL_i^2} \right] v_{i-1} + \left[\frac{GA_p h_a^2}{aL_{i+1}^2} \right] v_{i+1} \quad (1)$$

Where: v_{i-1} and v_{i+1} are the maximum displacements at the top of the piers $i-1$ and i .

The inertia force at the top of the pier depending on the displacement v_i is obtained by means of the following Eq. (2):

$$F_i^{in} = \frac{1}{\left[\frac{L_p^i}{K_i^s} + \frac{(L_p^i)^3}{3E_{ci}I_i} \right]} \left[v_i - \frac{2(q_i^{in})^{max} + (q_i^{in})^{min}}{6K_i^s} (L_p^i)^2 \right] - \frac{11(q_i^{in})^{max} + 4(q_i^{in})^{min}}{120E_{ci}I_i} (L_p^i)^4 \quad (2)$$

where K_i^s is the equivalent stiffness of the soil, $(q_i^{in})^{max}$ and $(q_i^{in})^{min}$ are the maximum and minimum inertial loads by unit length produced by the horizontal acceleration, in F_i^{in} is the total inertial force of the superstructure (girders) and L_p^i , E_{ci} and I_i are the length, Young’s modulus and the inertia of the pier cross section respectively.

At the top of each pier of the bridge, the total effective force is the sum of the forces R_i , produced by the rotation of the girders, given by Equation 1, with the forces F_i^{in} due to the displacement of the pier, given by Eq. (2). By applying now Newton’s second law, the total effective force at the top of pier i is

$$F_i^T = R_i + F_i^{in} = m_i a_i \quad (3)$$

Where m_i is the mass associated with the degree of freedom i, and a_i is the corresponding acceleration. Substituting the values of R_i and in F_i^{in} into Equation 3, F_i^T is expressed as

$$F_i^T = m_i a_i = \left\{ \left[\frac{GA_p h_a^2}{aL_i^2} + \frac{GA_p h_a^2}{aL_{i+1}^2} \right] + \frac{1}{\left[\frac{L_p^i}{K_i^s} + \frac{(L_p^i)^3}{3E_{ci}I_i} \right]} \right\} v_i - \left[\frac{GA_p h_a^2}{aL_i^2} \right] v_{i-1} - \left[\frac{GA_p h_a^2}{aL_{i+1}^2} \right] v_{i+1} - \left[\frac{1}{\left[\frac{L_p^i}{K_i^s} + \frac{(L_p^i)^3}{3E_{ci}I_i} \right]} \right] \left[\frac{2(q_i^{in})^{max} + (q_i^{in})^{min}}{6K_i^s} (L_p^i)^2 \right] + \frac{11(q_i^{in})^{max} + 4(q_i^{in})^{min}}{120E_{ci}I_i} (L_p^i)^4 \quad (4)$$

Defining from here the stiffness terms

$$K_{i,j} = \left[\frac{GA_p h_a^2}{aL_i^2} + \frac{GA_p h_a^2}{aL_{i+1}^2} \right] + \frac{1}{\left[\frac{L_p^i}{K_i^s} + \frac{(L_p^i)^3}{3E_{ci}I_i} \right]} \quad (5)$$

$$K_{i,i-1} = \left[\frac{GA_p h_a^2}{aL_i^2} \right] \quad (6)$$

$$K_{i,i+1} = \left[\frac{GA_p h_a^2}{aL_{i+1}^2} \right] \quad (7)$$

$$F_i^q = \left[\frac{1}{\left[\frac{L_p^i}{K_i^s} + \frac{(L_p^i)^3}{3E_{ci}I_i} \right]} \right] \left[\frac{2(q_i^{in})^{max} + (q_i^{in})^{min}}{6K_i^s} (L_p^i)^2 \right] + \frac{11(q_i^{in})^{max} + 4(q_i^{in})^{min}}{120E_{ci}I_i} (L_p^i)^4 \quad (8)$$

The final equilibrium equation can be written for each pier as $F_i^q + m_i a_i = K_{i,j} v_i - K_{i,j-1} v_{i-1} - K_{i,j+1} v_{i+1}$ (9)

Applying this equation to each degree of freedom of the structure, a system of equations $F = K v$ is obtained, where K is a tri-diagonal stiffness matrix, F is the force vector and v the displacement vector. As the transversal displacements at the girder-abutment connection are neglected, the final stiffness matrix of the bridge is of size $(n-2) \times (n-2)$, being n the number of piers and abutments of the bridge.

V. NON-LINEAR FORMULATION OF THE RC BRIDGE MODEL

In elastic conditions, the solution of Eq. (9) assures equilibrium at each time instant. However, when the non-linear behavior of the structural materials is taken into account, the equation of motion for each pier is written as

$$F_i^q + m_i a_i = K_{i,j} v_i - K_{i,j-1} v_{i-1} - K_{i,j+1} v_{i+1} - F_i^R \quad (10)$$

Where F_i^R is the residual force. This unbalanced force is due to the fact that the stiffness coefficients $K_{i,i}$, $K_{i,i-1}$ and $K_{i,i+1}$ are not constant and consequently the solution of Equation 10 should be obtained through an iterative process.

To obtain the maximum damage for the bridge piers using the model described in Fig. 4a, the non-linear Eq. (10) is solved using Newark’s algorithm. In this analysis the balance condition is achieved by eliminating F_i^R by means of a Newton-Raphson process, which indirectly eliminates the residual bending moment, ΔM , which is the difference between the maximum external moment, M_e , and the internal capacity, M_{int} , which is defined as structural capacity (C).



For each step of the non-linear analysis the properties of the system are updated, considering the degradation of the material caused by the seismic action, which is known as structural demand (D).

In the following the evaluation of the damage in the direction perpendicular to the bridge axis will be developed for any of the piers of the bridge, without a sub-index being written for the pier. Knowing the maximum displacement of a pier, the resultant force at the top and the maximum external moment at the base (predictor moment) can be obtained by means of

$$F_e = v k \quad (11)$$

$$M_e = F_e L_p \quad (12)$$

$$k = 3E_c I / L_p^3 \quad (13)$$

is the initial bending stiffness of the pier, F_e is the elastic force produced by any external action at the top of the pier, M_e is the maximum external moment, v is the maximum displacement of the pier (obtained by means of Newark's algorithm) and E_c , I and L_p are the Young's modulus of the concrete, the inertia of the cross section and the length of the pier, respectively. On the basis of the maximum external moment, it is possible to calculate the maximum damage that a pier can suffer due to seismic action.

In the case of seismic loads acting in the transversal direction of the bridge (x_1 axis), the elastic state of stress and strain in the longitudinal direction of the pier is

$$\varepsilon(x_1, x_3) = X_1(x_3) x_1 \quad (14a)$$

$$\sigma(x_1, x_3) = E_c \varepsilon(x_1, x_3) \quad (14b)$$

$$\text{Where: } X_1(x_3) = \frac{M_e(x_3)}{E_c I} \quad (15)$$

is the curvature of the pier, σ and ε are the stress and strain values, X_1 is the distance (in the direction of this axis) from the current point to the neutral axis of the cross section of the pier (see Fig. 4c), E_c is the initial Young's modulus of the pier, and M_e is the maximum external moment acting on the element.

Substituting Eq. (15) into Eqs. (14a),(14b), the cross sectional states of stress and strain in direction x_1 are defined by

$$\varepsilon(x_1, x_3) = \frac{M_e(x_3)}{E_c I} x_1 \quad (16a)$$

$$\sigma(x_1, x_3) = \frac{M_e(x_3)}{I} x_1 \quad (16b)$$

On the basis of these equations, the internal moment for the cross section of a pier is given by:

$$M_{int}(x_3) = \int_{A_c} \sigma x_1 dA_c \quad (17)$$

Where the internal moment in the longitudinal direction, $M_{int}(x_3)$, is obtained by integrating the moments of elements of the elemental forces σdA_c on the cross sectional area, A_c of the pier.

When the pier remains within the elastic range, its internal and external bending moments are equal. However, when the yield limit of the material has been exceeded, the demanded moment, M_e , is greater than the resisting moment, M_{int} , and the residual moment is

$$\Delta M(x_3) = M_e(x_3) - M_{int}(x_3) \quad (18)$$

This should be less than an imposed tolerance.

When the pier suffers damage, the state of stress developed in the damaged cross section of the structure (Eq. (16)) is evaluated by means of the following equation:

$$\sigma(x_1, x_3) = f(x_1, x_3) E_c^d X_1(x_3) x_1 \quad (19)$$

$$\text{Where: } E_c^d = f(x_1, x_3) E_c^0 \quad (20)$$

Is the Young's modulus of the damaged material, E_c^0 is the undamaged Young's modulus, and $f(x_1, x_3)$ is the damage function (which will be used to determine the probability of failure and Damage Index (DI)), that gives the probability that the seismic demand will exceed the structural capacity that was presented by others researchers Eunsoo Choi et al., Nielson and DesRoches)[5,7], which will be defined later. Substituting Eq. (19) into Eq. (17), the internal moment of the cross section of the pier is

$$\text{Where: } M_{int}(x_3) = E_c^0 X_1(x_3) I^d(x_3) \quad (21)$$

$$\text{Where: } I^d(x_3) = \int_{A_c} f(x_1, x_3) x_1^2 dA_c \quad (22)$$

is the inertia of the damaged cross section of the pier respecting the new neutral axis. For each time increment, a predictor moment is defined by means of the following equation:

$$M^0(x_3) = E_c^0 I(x_3) X_1(x_3) \quad (23)$$

In which the elastic properties of the material have been used.

For each time increment in which the predictor moment produces an unbalanced load increment greater than a tolerance (Eq. (18)), the procedure considers an increment in the curvature in order to obtain a corrector moment which permits it to reach the equilibrium state. The convergence criterion used states that the stable response is obtained for the whole structure if

$$C_c = \sqrt{\frac{\sum_i \Delta M_i^2}{\sum_i (M_i^e)^2}} \leq \text{TOL} \quad (24)$$

Where: TOL is the tolerance adopted (TOL \rightarrow 0).

The structural damage can be characterized at a given point and it is a reliable method of estimating the damage accumulation caused by a local micro-structural degradation obtained from the Continuum Mechanics, [16]. In order to define the inertia and the internal moment of the damaged cross section of a pier, the isotropic damage model of Oller et al. [16], has been applied. According to this model, the level of damage of the cross section of a pier is evaluated by means of the following damage function:

$$f(x_1, x_3) = 1 - d(x_1, x_3) \quad (25)$$

Where:

$$d(x_1, x_3) = 1 - \frac{\tau^*}{\tau(x_1, x_3)} \exp \left[A \left(1 - \frac{\tau(x_1, x_3)}{\tau^*} \right) \right] \quad (26)$$

Where τ is the current effective stress, τ^* the effective stress threshold, and A a parameter depending on the fracture energy. The inertia tensor of the damaged cross section is calculated by means of a numerical algorithm.

Once the convergence of the process is reached and the damage is calculated at each integration point, the maximum damage at the base cross section of a pier can be obtained. Two pier damage indices and three global damage indices are used in this paper. The first pier damage index characterizes the maximum damage at the base of each pier of the bridge

$$DI = \frac{M_e(x_3) - M_{int}(x_3)}{M_e(x_3)} \quad (27)$$

Using the pier damage index in Eq. (27) the global structural damage caused by seismic action in the bridge is described; a global mean damage index is defined as the average of the pier damage indices

$$D_m = \frac{\sum_i D_i}{n_p} \quad \text{Where: } (i=1, \dots, n_p) \quad (28)$$

Where: n_p is the number of piers of the bridge.

Established fragility curves are constructed with respect to PGA. The damage ratio for each damage rank at each excitation level is obtained by calibrating the DI using Table 1. Based on this data, fragility curves for the bridge piers are derived assuming a lognormal distribution.

VI. VERIFICATION OF SIMPLIFIED MODEL

In the numerical analysis the study present 3D finite element model for the bridge with full detail using the Drain 2X code and the simplified finite element model based on the above mentioned sections. The two models were analyzed under the same factored ground excitation of El-Centro, 1940 to verify the accuracy of the new proposed simplified model. Fig. 4a presents the frame elements and joints for the finite model. The soil simulation was presented in both cases and simulated as springs in all direction with rotational stiffness as per Lysmer and Richard [17]. Figs. 5a, 5b show a comparison in which the dynamic response of simplified proposed model and numerical finite element model of studying bridge which was shacked to factored real earthquake El-Centro, 1940. It should be mentioned that, the comparison is conducted for both pier displacement time history and shear hysteretic loop.

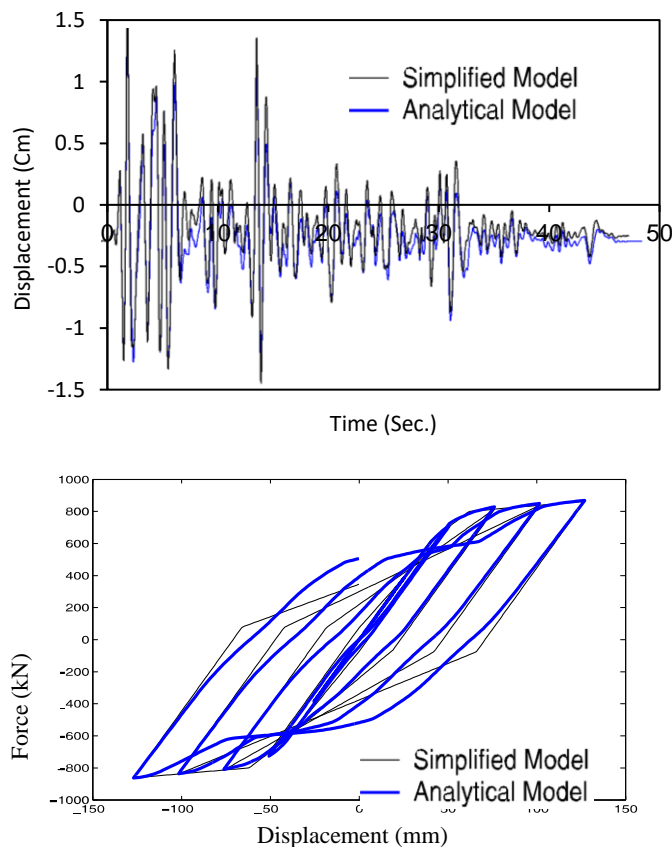


Fig. 5b Comparison of force –displacement relationship (Hysteretic shear loop) of the simplified model versus to the 3D model of bridge.

It is worthwhile to mention that these results were obtained when the bridge was subjected to scaled factored ground excitation of El-Centro, 1940. The factor ratio equal to the peak ground acceleration of Al-Aqba, 1995 to the peak acceleration of El-Centro, 1940, as shown in (Figs. 3a, b, c, and d). As shown in (Figs. 5a, 5b), the comparison is very satisfactory with results are in a very good agreement in both time history of displacement and hysteretic shear loop, respectively.

That means success of the simplified proposed model and trusting for its results in the further dynamic analysis

VII. NON-LINEAR ANALYSIS AND FRAGILITY CURVE

The fragility curves obtained by this approach consider both structural parameters and variation of input ground motion.

The steps for constructing the analytical fragility curves are as follows:

1. Select the earthquake ground motion records.
2. Normalize PGA of the selected records to different excitation levels.
3. Make an analytical model of the structure.
4. Obtain the stiffness of the structure.
5. Select a hysteretic model for the non-linear dynamic response analysis.
6. Perform the non-linear dynamic response analysis using the selected records.
7. Obtain the ductility factors of the structure (μ).
8. Obtain the damage indices of the structure in each excitation level.
9. Calibrate the damage indices, (DI) for each damage rank, (DR).
10. Obtain the number of occurrences of each damage rank in each excitation level and get the damage ratio.
11. Construct the fragility curves using the obtained damage ratio and the ground motion indices for each damage rank.

The ductility factor μ at the top of the bridge pier is obtained from non-linear dynamic response analysis. The total ductility demand is calculated considering both displacement and hysteretic energy ductility. The hysteretic energy ductility is considered as it contributes a significant damage to the structure. The displacement ductility μ_d is defined as the ratio of the maximum displacement (obtained from dynamic analysis) to the displacement at the yield point (obtained from static analysis). In a similar way, the hysteretic energy ductility μ_h is defined as the ratio of the hysteretic energy to the energy at the yield point. The ductility factors thus obtained are used to evaluate the damage of the bridge piers.

VIII. ANALYTICAL FRAGILITY CURVES OF EGYPTIAN RC PIER BRIDGE

Fragility analysis for highway bridges has become increasingly important in the risk assessment of highway transportation networks exposed to seismic hazards. Analytical fragility curves are developed though seismic response data from the bridges analysis.

The fragility curve analysis generally includes three major parts:

1. The ground motion Excitation, so the paper used many time histories of earthquakes including the only available Egyptian record of Al-Aqba, 1995, also the rescaling for the others international earthquakes in trial to be matched with the zone excitation of motion.

Even having the same PGA and PGV, it is assumed that structural damage due to different records from different earthquakes might be different. This is due to the characteristics (frequency contents, phase, duration, etc.) of the input ground motion.

The acceleration time histories were chosen on the basis of large peak ground acceleration (PGA) values. Both the EW and NS components are employed to generate a large number of records. Using these acceleration time histories as an input motion, the damage indices of the bridge piers are obtained from the non-linear analysis. Finally, using the obtained damage indices and the ground motion indices, the analytical fragility curves for RC bridge piers are constructed.

2. The simulation of bridge to account for uncertainty in bridge properties; that was done and verified with the full details 3D bridge model with the new simplified proposal model to trust the results.

3. The generation of fragility curves shall be taken from the seismic response data of bridges. The seismic response data can be obtained from nonlinear time history analysis.

Fig. 6 presents the construct analytical fragility curve of the Egyptian RC bridge case study that was presented in the paper. The figure presents the probability of damage versus to the damage indices for different peak ground excitation from 0.15g up to 0.4g that can be consider suitable and enough to the case study zone moderate and weak earthquake zone.

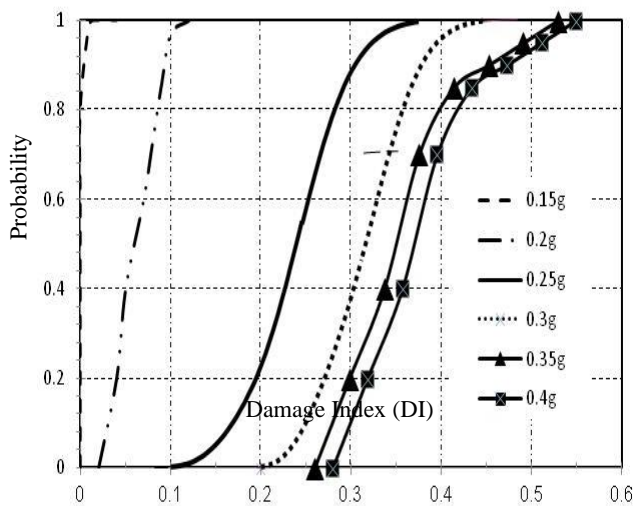


Fig. 6 Fragility curve of RC pier bridge type of EGARB in Egypt.

In Fig. 6 the curves associated with peak ground acceleration of 0.15g and 0.2g is slightly damage that means the pier concrete section has a linear behavior for these ground acceleration scale. For peak ground acceleration value greater than 0.25g to 0.3 g the pier behavior can be consider as moderate damage and the pier section will be need for enhancement procedure especially for the moderate seismicity zone area in Egypt like north coast of the

Mediterranean Sea and east of Suze Gulf and Al-Aqba Gulf. For others peak ground acceleration value greater than 0.35 g the pier will be suffered from severe damage for this earthquake excitation and pier concrete section will be not safe and may be will subject to sudden shear failure.

Based on the final fragility curve for the RC pier bridges, the Egyptian General Authority of Roads and Bridges (EGARB) can be reevaluate the enhancement plan for these pier bridges based on the design PGA value and This can be used for prioritizing retrofit, pre-earthquake planning, and loss estimation tools.

IX. CONCLUSION

In Egypt, neither bridge damages nor their performance have been reported during the previous earthquakes. According to that, this paper proposes a seismic vulnerability evaluation method based on structural nonlinear analysis for RC bridges with simple pier bents. The proposed model is based on the characterization of the maximum damage of the piers of the bridge, the damaged inertia being obtained at their base. It is calibrated using a Finite Element (FE) model.

The paper success to present easy, accurate, and new analytical propose method to get on the fragility curve of the all most typical and repeated Egyptian RC pier bridge. The presented fragility curves describe the probability of structure being damaged beyond a specific damage for various levels of ground excitation. This will be used for prioritizing retrofit, pre-earthquake planning, and loss estimation tools. This is particularly useful in regions of moderate seismicity, like Egypt.

This is particularly useful in regions of moderate and slightly seismicity, such as Egypt and the Middle East area, where Egyptian General Authority of Roads and Bridges (EGARB) are being to develop retrofit programs, in additional to conducting pre-earthquake planning.

The author recommend to add the fragility curve in the new version of Egyptian loading code practice ECP 201, where all the available revisions are still missing this important technique for the bridge design.

REFERENCES

- [1] S. A. Kurian, S. K. Deb, and A. Dutta, "Seismic vulnerability assessment of a railway over bridge using fragility curves," Proceeding of 4th International Conference on Earthquake Engineering, Taipei, Taiwan, 2006.
- [2] M. L. Seongkwan, J. K. Tschangho, and L. K. Seung, "Development of fragility curves for bridges in Korea" KSCE Journal Civil Engineering 2007, 3(11),pp165-174.
- [3] J. E. Padgett, and R. DesRoches, "Methodology for the development of analytical curves for retrofitted bridges," Earthquake Engineering Structural Journal 2008, 37, pp.1157-1174.
- [4] I. F. Moschonas, A. J. Kappos, P. Panetsos, V. Papadopoulos, T. Makarios, and P. Thanopoulos, " Seismic fragility curves for greek bridges: methodology and case studies," Bull. Earthquake Engineering 2009, 7, pp.439-468.
- [5] Eunsoo Choi, Reginald DesRoches, and Bryant Nielson, "Seismic fragility of typical bridges in moderate seismic zones," Engineering Structural journal 2004, 26, pp.187-199.
- [6] Qi'ang Wang, Ziyang Wu, and Shukui Liu, "Seismic fragility analysis of highway bridges considering multi-dimensional performance limit state," Earthquake Engineering and Engineering Vibration 2012; 11(2):185-193, (DOI: 10.1007/s11803-012-0109-1).

- [7] B. Nielson, and R. DesRoches , "Analytical seismic fragility curves for typical bridges in the central and south eastern United States," *Earthquake Spectra Journal* 2007, 3(23),pp.615-633.
- [8] Y. J. Park, and A. H. S. Ang, "Seismic damage analysis of reinforced concrete buildings," *Journal of Structural Engineering*, (ASCE), 1985, 111(4), pp.740-757.
- [9] F. A. Charney," NONLIN – Nonlinear dynamic time history analysis of single degree of freedom systems," Federal Emergency Management Agency Training Center, Emmitsburg, Maryland, Advanced Structural Concepts, Golden, CO and Schnabel Engineering, Denver, Co, 1998.
- [10] J. B. Mander, and N .Basoz, "Seismic fragility curves theory for highway bridges," *Proceeding of 5th U.S. Conference of Lifeline Earthquake Engineering*, ASCE, 1999, pp. 31-40.
- [11] A .Ghobarah, N. M. Aly, and M. El-Attar, "Performance level criteria and evaluation," *Proceeding of the International Workshop on Seismic Design Methodologies for the Next Generation of Codes*, Balkema, Rotterdam, 1997, pp. 207-215.
- [12] H. Hwang, B. L. Jing, and Y.Chiu," Seismic Fragility Analysis of Highway Bridges," Ref. No. MAEC RR-4, Center for Earthquake Research Information, Memphis, 2001.
- [13] ECP-201 Permanent Committee, ECP-201:1993, ECP-201:2003, and ECP-201:2008. Egyptian Code for calculating loads and forces in structural work and masonry. HBRC, Giza, 1993, 2003, and 2008(Draft), respectively.
- [14] V. Prakash, G.H. Powell, S.D. Campbel, and F.C. Filippou, "DRAIN-2DX user guide," Department of Civil Engineering, University of California, Berkeley, 1992.
- [15] E.C. Bentz, and M.P. Collins," Response-2000. Software Program for Load-Deformation Response of Reinforced Concrete Section," 2000 (<http://www.ecf.utoronto.ca/bentz/inter4/inter4.shtml>).
- [16] S. Oller, A. H. Barbat, E. Onate, and A. Hanganu, "A damage model for the seismic analysis of buildings structures," *10th World Conference on Earthquake Engineering*, 1992, pp. 2593-2598.
- [17] J. Lysmer, and F. E. Richart," Dynamic response of footings to vertical loading," *Journal of the soil Mechanics and foundations Division*, ASCE, 1966, 92 SMI.



Islam M. Ezz El-Arab is a assistant professor of structural engineering Department at Tanta University. He obtained his Ph.D and M.Sc. in Earthquake Engineering area and Dynamic of Structures. He has many technical papers related to the behaviour of reinforcement concrete structure under seismic excitation, and structures dynamic performance.

Ezz El-Arab is a member of several professional committees in Egypt and abroad like the Egyptian civil syndicate, Egyptian Society for Earthquake Engineering, Federation of Arab Engineers, (member ship No. 16/20384), Saudi Council of Engineers, (KSA) (Professional Engineer), (member ship No. 76206), and Egyptian Engineering Association in Riyadh, KSA, (member ship No. 1016/2010).